A Unified Stochastic Volatility - Stochastic Correlation Model

Xiang Lu lvxiang@hawaii.edu

Gunter Meissner meissner@hawaii.edu[1]

Hong Sherwin hongsherwin@gmail.com[2]

Abstract

This paper has two main contributions. First, we build a simple but rigorous stochastic volatility – stochastic correlation model. Mean-reverting and locally stochastic with dependent Brownian motions, our model proves to fit both marginal and joint distributions of the option market implied volatility and correlation.

Second, asset correlations are currently modeled exogenously and then ad hoc assigned to an asset price process such as the Geometric Brownian motion (GBM). This is conceptually and mathematically unsatisfying. We apply our approach to build a unified asset price - asset correlation model, which outperforms the standard GBM significantly.

Keywords: stochastic volatility, stochastic correlation, CKLS, CEV, CIR, Jacobi

JEL Classification: C12, C32

[1] Corresponding Author
[2] Corresponding Author

1. Introduction and Motivation

Asset prices are typically modeled with the Geometric Brownian motion (GBM) of the form

$$dS_t/S_t = \mu\, dt + \sigma\, dB_t \quad (1)$$

where S_t is the asset price, μ is the drift, σ is the volatility, and dB_t is a standard Brownian motion.

Rapid developments in vanilla and exotic options markets, over the past several decades, have fundamentally challenged the static assumptions of μ and σ parameters in GBM. Merton [33] introduces jumps and shows that if the logarithm of the percentage jump is normally distributed, a closed form solution for European style options exists. Cox and Ross [16] create the constant elasticity of variance (CEV) model, where an exponential parameter α added to the asset price. The value of α determines the dependence between asset price and volatility. In a pure jump extension, Madan et al. [33] follow a variance-gamma approach, which create heavier tails and provides semi-analytic expressions for European style options.

Heston [23] in a seminal model correlates the asset return process with stochastic variance. Many Heston model extensions have since developed with Zhou [37], Hagan et al. [22], Brigo and Pallacinini [6], and Langnau [27] counted among many prominent examples.

The availability of market data of implied volatility surface[3] has ushered in a new era of stochastic volatility modeling to reproduce a multitude of finer properties observed in the real world. Cont et al. [14] prove that 1-factor model is insufficient to represent the true dynamics in the observed SPX volatility surfaces. Furthermore, the eigenfactors of the vol-surface time series are found not to be perfectly correlated to

[3] The 3-D surface $\sigma_t^{BS}(K,T)$ is implied from vanilla option prices via Black-Scholes-Merton formula, with strike K and maturity T.

the underlying asset price movements – hence concluding - `Vega' risk cannot be reduced to `Delta' risk.

In a series of ground-breaking papers, Bergomi [5] and others set out to capture the term-structure of skew and vol-of-vol in a Forward Variance Swap framework, creating an analog of the Libor Market Model. A class of models has since multiplied aimed to price the exotic contracts consistently to vanilla options, therefore solving the `Joint S&P/VIX Smile Calibration Puzzle'. By adding simultaneous jumps to the Ornstein-Uhlenbeck process of the Forward Variance Swap and the underlier GBM process, the flexible Lévy specification by Cont et al. [15] offers a greater analytical tractability and more efficient control of the volatility-skew and the shifting correlation between spot and implied volatility.

Academic interests between asset volatility and asset correlation have been uneven, although the need for a joint and consistent framework arises not only for asset pricing, portfolio construction but also for derivatives pricing and risk distribution. In comparison to stochastic volatility, we argue that far less progress has been made in the literature in modeling asset correlation as a state-dependent market risk factor.

Studies of realized stock correlations should help shed light in this important research area. The summary statistics in Table 1 reveals that the level and variability of cross-sectional asset correlation both move higher conspicuously when market is in distress, from a distinctly mild regime observed during expansionary economic times. Meissner [31] further asserts that elevated correlations persist without necessarily accompanied by rising volatility during recessionary periods.

	Avg Stock Correlation	
Economic Condition	Level	StdDev
Expansionary	27.46%	71.17%
Normal	33.19%	82.51%
Recessionary	36.96%	80.48%

Table 1: Stock Correlation Level and StdDev
from Jan. 1972 to Mar. 2020[4]

[4] Correlations estimated are the average of Pearson 30x30 correlation matrix of Dow Index stock price returns.

Analogous to the irreducible `Vega' risk in the Implied Volatility (IV), the empirical evidence clearly supports the role of the Implied Correlation (IC) as a unique source of randomness to the financial system.

Hull et al. [26] model the asset process in a GBM setting and then sample the asset correlation from a beta distribution, with the distribution parameters exogenously derived and not time-varying. Ma [29] models stochastic volatility and stochastic correlation processes to price exchange rate options, and Ma [30] applies stochastic correlation to price and hedge multi-asset options, the volatility and correlation are however assumed independent from each other.

Emmerich [20] highlights the unique mathematical properties of a stochastic correlation process. Düllman et al. [19] model stochastic correlation with a Vasicek process. However, both papers do not combine the correlation process with the asset process.

Buraschi et al. [8] and Fonseca et al. [21] extend the Heston [23] model, by correlating a n-dimensional stochastic correlation process with a n-dimensional stochastic asset process.

The `correlation' term is applied ubiquitously within and across a variety of risk factors, it should be noted that the asset correlation in our study is restricted to the equity price returns. In contrast to Burtschell et al. [9], the local stochastic correlation model targets the default time correlation within a portfolio of Credit Default Swaps (CDS) instead.

The remaining paper is structured as follows: In section 2 we introduce our unified stochastic asset volatility – stochastic asset correlation model. In section 3 we show the real world fit of the model. Section 4 discusses the calibration of the eight parameters. Section 5 conducts the significance tests. Section 6 applies the model in an enhanced version of GBM.

2. The USVSC Model

Our proposed Unified Stochastic Volatility – Stochastic Correlation model (USVSC henceforth) consists of three stochastic differential equations:

$$\begin{cases} d\sigma_t = \kappa_\sigma(m_\sigma - \sigma_t)dt + \nu_\sigma \sigma_t^\beta dW_t & (2) \\ d\rho_t = \kappa_\rho(m_\rho - \rho_t)dt + \upsilon_\rho\sqrt{1-\rho_t^2}\, dZ_t & (3) \\ dW_t = \rho_w dZ_t + \sqrt{1-\rho_w^2}\, dZ_t^\perp & (4) \end{cases}$$

where stochastic instantaneous volatility σ_t and stochastic instantaneous correlation ρ_t are set within a local volatility framework, mean-reverting with a rate of $\kappa_{\{\sigma,\rho\}}$ to a long-term mean of $m_{\{\sigma,\rho\}}$. The diffusion coefficient is denoted as $\nu_{\{\sigma,\rho\}}>0$, and the positive skew in σ_t is captured by a power parameter β. The modeled stochasticity is generated by three 1-dimensional standard Brownian motions $\{W_t, Z_t, Z_t^\perp\}$, where Z_t and $Z_t^\perp$ orthogonal, W_t and Z_t correlated with a coefficient ρ_w.

Eq (2), referred to as CIRCEV hereafter, extends the Cox-Ingersoll-Ross (CIR) model with a β exponent parameter, otherwise known as Chan-Karolyi-Longstaff-Sanders (CKLS) model proposed by Chan et al. [13], or a variant of the Constant Elasticity of Variance (CEV) model. Evoking CIRCEV model specification is motivated by its non-negativity and mean-reversion properties fitting the implied volatility, and the presence of a positive skew found empirically and prominently displayed in Fig (1c).

Eq (3) specifies a Jacobi process, otherwise known as Wright-Fisher diffusion process. Jacobi is a natural model choice for implied correlation, in which not only the mean-reverting empirical feature is preserved, the limiting behavior for a correlation is also obeyed naturally at -1 or +1. As discussed by Ahdida et al. [1], Emmerich [20] and Zetocha [36], Jacobi specification permits analytical solutions of the first two moments, as well as the average over an arbitrary length of time. Although, like Heston [23], a Feller-like inequality constraint should apply over model parameters to ensure the desired numerical stability.

Eq (4) gives a dependence structure between the implied volatility and the implied correlation, analogous to Heston [23] in treating the joint distribution between spot and local variance.

In summary, our USVSC model is formulated as a correlated CIRCEV and Jacobi processes in an attempt to capture the equity derivatives dynamics. The rational for disallowing the joint-dynamics between derivatives and underlying spot market is two-fold: a) to keep the model at the lowest possible dimension in support of historical calibration; and b) to expose the risk factors exclusively within derivatives, as opposed to a joint model traditionally done for efficient hedging purpose.

Our model consists of a total of eight parameters, namely, $\Theta = \{\kappa_\sigma, m_\sigma, \nu_\sigma, \beta, \kappa_\rho, m_\rho, \nu_\rho, \rho_{\mathbf{w}}\}$, forming the set of unknowns to be estimated empirically, with a goal to better understand the historically realized marginal and joint distributions of the risk neural option implied volatility and implied correlation through time.

3. Real World Fit

CBOE publishes both historical data series of the Implied Volatility (known as the VIX - the "fear gauge"), and the Implied Correlation, derived from vanilla SPX options and dispersion trading strategies respectively, following the estimation methodologies given by CBOE [10] and CBOE [11].

To measure the efficacy of our model and demonstrate an actual calibration implementation, we let VIX represent IV (the option-implied volatility σ_t), and the CBOE Implied Correlation as IC (the option-implied correlation ρ_t). Our dataset is comprised of the SPX, the VIX and the ICJ/JCJ indexes observed from 01/03/2007 to 08/01/2019, daily sampled and sourced from www.CBOE.com.

Strictly speaking, the VIX only corresponds to the estimated implied volatility of 30-day SPX OTM call/put contracts through a convergence framework between variance swap pricing and log-Price option contract. In order to model VIX Options and Futures over tenor T, consistently with SPX options, it is most common to express VIX as the

integral of an instantaneous forward variance rate $\tilde{\sigma}^2_{t,t+T}$, as in Cont et al. [15] and Bergormi [5], rather than the instantaneous volatility stochastic factor σ_t as we proposed in Eq (2).

$$VIX_t = \tilde{\sigma}_{t,t+T} = \sqrt{\frac{1}{T}\int_t^{t+T} \tilde{\sigma}^2_{t,u} du}$$

With respect to the quantity of ρ_t in Eq (3), a similar expression exists for Implied Correlation (IC) derived from the termed implied volatility of SPX index $\tilde{\sigma}_{t,t+T}$ and that of a single stock $\tilde{\sigma}_{j,t,t+T}$, extended from Driessen et al. [18]:

$$\tilde{\rho}_{t,t+T} = \frac{1}{T}\int_t^{t+T} \tilde{\rho}_{t,t+u} du = \frac{1}{T}\int_t^{t+T} \frac{\tilde{\sigma}^2_{t,u} - \sum_{j=1}^{N} w^2_{j,t}\tilde{\sigma}^2_{j,t,u}}{\sum_{j,l\neq j}^{N} w_{j,t}w_{l,t}\tilde{\sigma}_{j,t,u}\,\tilde{\sigma}_{l,t,u}} du$$

where $w_{j\in\{1,\dots,N\},t}$ denotes the weight of j-th single stock in the index at time t, and T=30 days in the case of CBOE indexes.

To simplify the calibration, without evoking the stochastic instantaneous forward variance curve nor the required stochastic instantaneous forward correlation curve, we implicitly assume $\sigma_t := \tilde{\sigma}_{t,t+T}$ and $\rho_t := \tilde{\rho}_{t,t+T}$ for illustration purpose. Essentially a 1-month forward term-structure is embedded in both stochastic variables of IV and IC. This slight abuse of notation is acceptable, since i) T is fixed at 30 days everywhere; and ii) the emphasis of our study is to uncover the systemic interactions between IC and IV, impacts from term-structure within 30 day, and the relevant refinements in `Delta', `Vega', `Skew' and `Vol-of-Vol' risk hedging strategies are left for future studies; and lastly iii) a fairly flat historical average term structure is reported in both IV and IC for tenors longer than 1-month, according to the summary statistics[5] of SPX option data from 1997 to 2015 in Hollstein et al. [24].

We first display the excellent real world fit of our model, which is followed by a detailed description of a 2-staged calibration and the correspondent statistical test results.

[5] Table 1 in Hollstein et al. [24] Online Appendix

Fig (1) describes historical properties of the Implied Volatility (IV) and the Implied Correlation (IC).

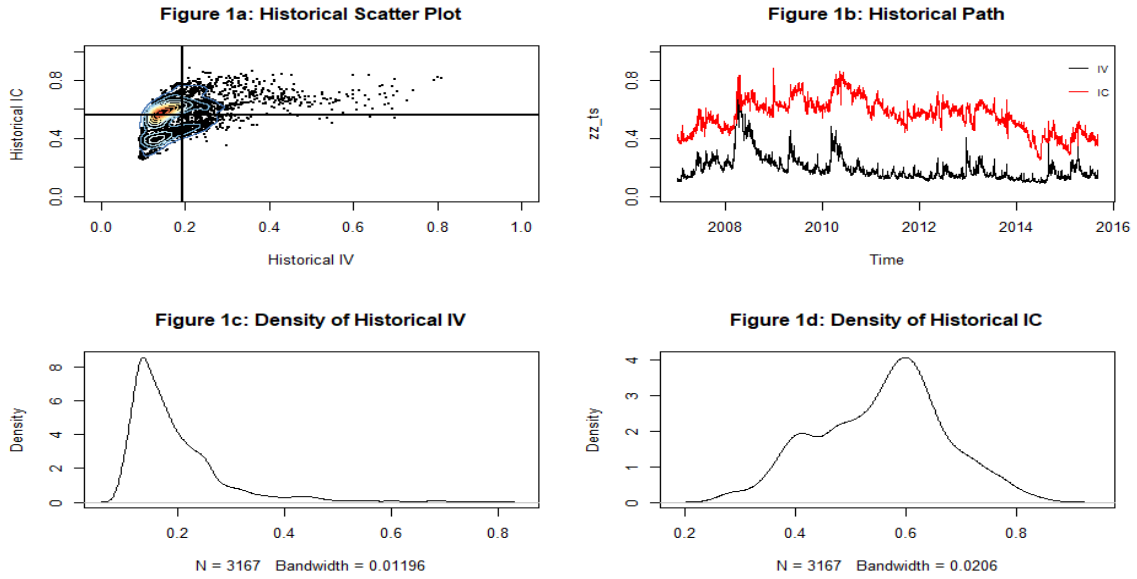

Figure (1a): Empirical relationship between IV and IC. Figure (1b): Time series plot of the empirical IV and IC. Figure (1c): Density of empirical IV. Figure (1d): Density of empirical IC

Fig (2) displays the simulated properties of the Implied Volatility (IV) and the Implied Correlation (IC) using our calibrated model results

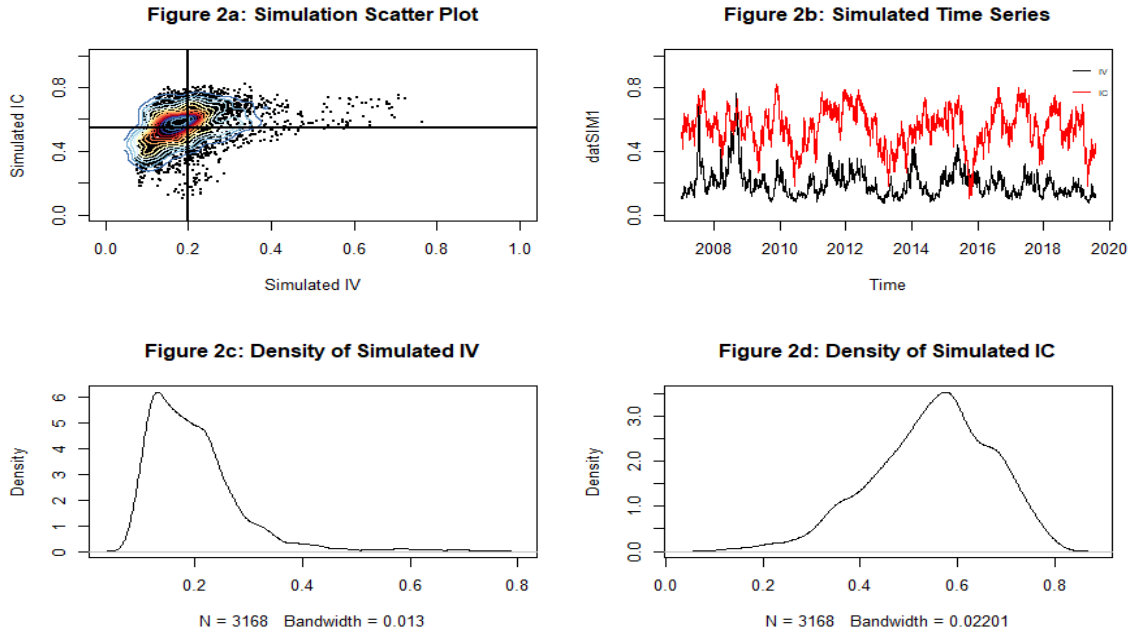

Figure (2a): Modeled relationship between IV and IC. Figure (2b): Time series plot of the modeled IV and IC. Figure (2c): Density of modeled IV. Figure (2d): Density of modeled IC

With respect to Fig (2a), the USVSC model is designed to produce a positive - 'triangular' relationship between IV and IC as shown in Fig (1a). A positivity in ρ_w is expected to enable synchronized co-movements between σ_t and ρ_t. Furthermore, as the correlation approaches upper or lower bounds, i.e. +1 or -1, its stochasticity decreases due to the diffusion term $\upsilon_\rho \sqrt{1-\rho_t^2}$ specified in Eq (3).

After outlining our calibration procedure in section 3, we perform a series of statistical tests associated with Fig (2a) to Fig (2d) in section 4.

4. Model Calibration

The estimation scheme is described in this section. We approach the calibration in three Stages using the Maximum Likelihood Estimation (MLE) framework. We believe MLE is simplest to implement, numerically stable while allowing for the generation of the desired statistical inferences.

4.1 Stage I – Marginal Distributions of IV and IC

By design of the proposed USVSC model, except for the correlated Brownian motions anchored by Eq (4), IV and IC have no interactions in the drift as well as the diffusion terms, divergent from that in Heston [23]. Under this specification, therefore, a decoupled and 1-dimensional historical calibration, separated for IV or IC process, is permissible.

To illustrate, we first suppose a generalized univariate stochastic differential equation (SDE) with drift and diffusion terms fully parameterized as follows:

$$\mathrm{d}X_t = \mathrm{f}(X_t, \theta)\mathrm{d}t + \mathrm{g}(X_t, \theta)dW_t \tag{5}$$

Where $\{X_t\}$ represents the time series of empirical observations, and Θ the collection of model parameters. We assume the increments of observations dX_t conditionally Gaussian $N(\mu_X, \sigma_X^2)$. This means, based on the Euler discretization scheme, we can derive

explicitly the first two moments of the increments, similar to the approach taken by Ait-Sahalia [2]:

$$\mu_X = \mathrm{E}(\Delta X_t) = f(X_t,\theta)\Delta t,\ \sigma_X^2 = \mathrm{E}\,[Var(\Delta X_t)] = g(X_t,\theta)^2\Delta t \quad (6)$$

The transition density, under our assumption, can therefore be expressed in a closed-form:

$$p_\theta(\Delta t, x_i\,|x_{i-1}) = \frac{1}{\sqrt{2\pi\Delta t g(x_{i-1},\theta)^2}}\exp[-\frac{(x_i - x_{i-1} - f(x_{i-1},\theta)\Delta t)^2}{2\Delta t g(x_{i-1},\theta)^2}] \quad (7)$$

The optimization objective function immediately follows, resulting in a maximization problem of the log-likelihood function to solve Θ:

$$\begin{aligned}\Theta &= \mathrm{argmax}_\theta\ \log[\Pi_{i=1}^N p_\theta(\Delta t, x_i\,|x_{i-1})] \\ &= \mathrm{argmax}_\theta\,\{-\log[2\pi\,\Pi_{i=1}^N g(x_{i-1},\theta)^2] + \sum_{i=1}^N \frac{(x_i - x_{i-1} - f(x_{i-1},\theta)\Delta t)^2}{2\Delta t g(x_{i-1},\theta)^2}\}\end{aligned} \quad (8)$$

With an unconstrained optimization routine[6], we first report in Table 2 the results of USVSC model parameter estimation of Θ, along with the corresponding estimation errors.

IV	Coeff	Std Error
$\widehat{\kappa_\sigma}$	7.1714	1.7569
$\widehat{m_\sigma}$	0.1940	0.0161
$\widehat{v_\sigma}$	2.2586	0.1364
$\hat{\beta}$	1.2296	0.0343

IC	Coeff	Std Error
$\widehat{\kappa_\rho}$	10.9385	1.3941
$\widehat{m_\rho}$	0.5548	0.0153
$\widehat{v_\rho}$	0.5984	0.0075

Table 2: Univariate Calibration of IV and IC

The calibrated parameters of IV, per Eq (2) - CIRCEV specification, including the long-term mean, the reversion rate (half-life), the magnitude in vol-of-vol, together with

[6] We thank Prof. Boukhetala for R package Sim.DiffProc and the useful discussions

the CEV skew parameter β > 1, are all of expected values with a good match to existing literature, such as Ait-Sahalia and Kimmel [3] and Bu et al. [7].

The calibrated parameters of IC, per Eq (3) - Jacobi process, are shown to have met the inequality condition of the mean-reverting rate, $\kappa_\rho \geq max\left(\frac{v_\rho^2}{1+m_\rho}, \frac{v_\rho^2}{1-m_\rho}\right)$, consistent to relevant discussions in Emmerich [20], Ma [29] and [30], as well as Zetocha [36].

To test the robustness, we produce 5k simulations to visualize in Fig (3). We confirm the fulfillment of correlation boundedness achieved by the calibrated parameters. In addition, the mean is fairly stable around the randomly assigned initial value of 0.2.

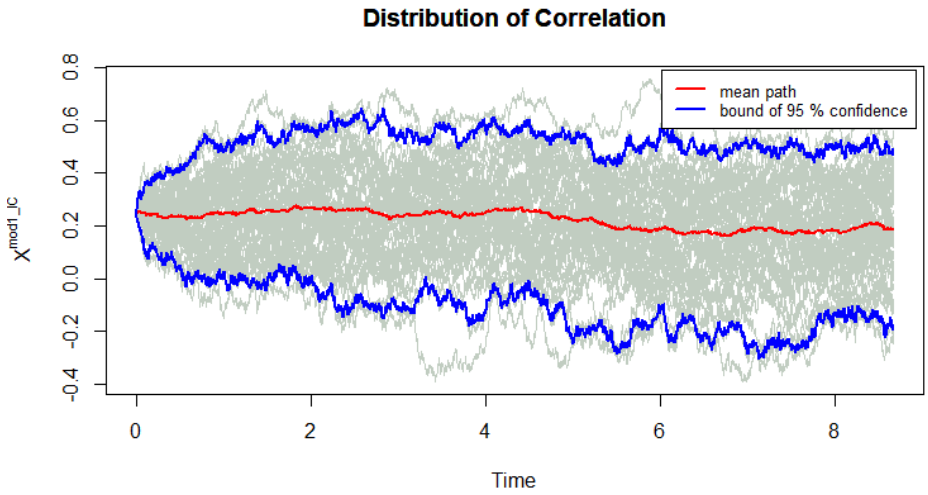

Figure (3): Time series of Simulated Implied Correlation

The red line in Fig (3) represents the time series mean of all simulated IC paths, which exhibits a relative stability as IC converges to a long-term mean prescribed by a Jacobi process as in Eq (3). Measured by each simulated single path shown in Fig (2b), and relative to IV, however, a greater magnitude of variability in IC empirically observed in Fig (1b) is largely captured, helped in part by a faster mean-reverting rate $\widehat{\kappa_\rho}$.

4.2 Stage II - Correlated Brownian Motions

Having estimated the seven parameter values in Θ , $\{\kappa_\sigma, \mu_\sigma, \upsilon_\sigma, \beta, \kappa_\rho, \mu_\rho, \upsilon_\rho\}$, required by the model, we now turn our focus to the eighth parameter ρ_w and the correlated Brownian motions in Eq (4).

We reconstruct the realized increments of Brownian motions, dW_t and dZ_t, making use of the estimated parameters from Stage I. Under the normality assumption, it follows that the asymptotic correlation coefficient estimation as specified in Eq (5) is just the expectation of the product of dW_t and dZ_t scaled by dt:

$$\rho_w = E\left(dW_t \times dZ_t\right)/dt \tag{9}$$

The estimated correlation coefficient parameter $\widehat{\rho_w}$, together with the t-statistic and p-value are presented in Table 3. The zero-value null hypothesis is strongly rejected at 95$^+$% confidence level. This is an important finding from our Stage II calibration.

H_0: $\rho_w = 0$

$\widehat{\rho_w}$	0.5056435
T	19.889
p-value	2.20E-16

Table 3: Correlation Calibration Result of p_w of Eq (4)

The histogram of the product of the white noises is displayed in Fig (4) for illustration purpose.

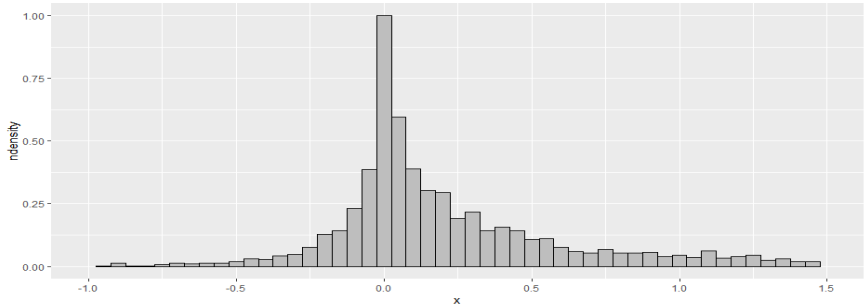

Figure (4): Histogram of $dW_t \times dZ_t/dt$

5. Goodness-of-Fit Tests

In this section, we test if our calibrated model is statistically accurate in representing the empirical data. The marginal distributions of IV and IC resulted from calibration Stage I are first examined, which are followed by normality tests concerning the correlation parameter ρ_w estimated in calibration Stage II.

5.1 Testing for Stage I

To test the equality in aggregation distribution between the historical IV and IC densities in Fig (1c) and Fig (1d), and our model-simulated densities in Fig (2c) and Fig (2d), we proceed as follows.

Firstly, we perform non-parametric Kolmogorov-Smirnov (KS) test for the difference in univariate distributions. With the cumulative distribution functions (CDF) denoted as F(IV) and F(IC), respectively, between the empirical distributions and the modeled 1-path time series simulation, denoted as $\hat{F}(\mathrm{IV})$ and $\hat{F}(\mathrm{IC})$, started with a pair of arbitrary points (IV_0 , IC_0). Below 5% are the max distances between two CDFs measured by the D-Scores associated with IV and IC. Nearing 1% p-values found by the tests, however, suggest the null hypothesis should be rejected with 95% confidence level.

$$H_0: F(IV) = \hat{F}(IV), \qquad F(IC) = \hat{F}(IC)$$

	IV	IC
D	0.0404	0.0483
p-value	0.0113	0.0013

Table 4: 1-path Kolomogorov-Smirnov (KS) test for equivalence between empirical and the simulated 1-path time series with an arbitrary starting point of IV_0 and IC_0

Secondly, we utilize a form of randomization test - the Permutation Test of Equality. With paired samples of univariate distributions, the high p-values registered for both IV and IC suggest a high degree of equality in distribution between the model generated IV or IC process and the correspondent empirical counterpart.

$H_0: F(IV) = \hat{F}(IV), \quad F(IC) = \hat{F}(IC)$

	IV	IC
H	0.0177	0.0238
p-value	0.9700	0.9860

Table 5: 1-path Permutation Test

Graphical depiction rendered in Fig (5) shows the density functions of IV and IC, respectively, between the simulated series and the empirical observations. The blue color identifies the largest distances in density, along the x-axis continuous values of likely (IV ϵ [0, +1]) and feasible (IC ϵ [-1, +1]) ranges. This should shed additional light on the locality of the discrepancies in the interest of future studies.

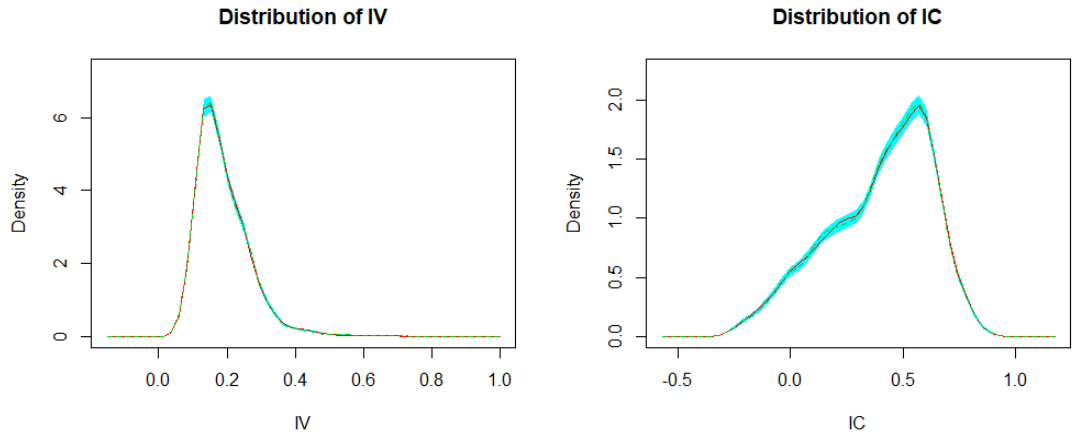

Figure (5): 1-path IV and IC Permutation Test

Lastly, we study the sensitivity of inference test results to the numerical noises embedded in Monte Carlo simulations. When the number of simulation paths increases, the replicability of the distribution by our parameterized model is expected to significantly improve. This effect can be demonstrated via an unpaired 2-sample Wilcoxon test, also known as Mann-Whitney test.

Judging by the large test statistics W and the high p-values (>>10%) reported in Table 6, resulted in by comparing 5k paths simulation against the single-path historical realizations, one can't reject the null hypothesis of identical distribution for both IV and IC at 95% confidence level.

$H_0: F(IV) = \hat{F}(IV), \quad F(IC) = \hat{F}(IC)$

Wilcoxon	IV	IC
W	2.48E+10	2.55E+10
p-value	0.2885	0.1113

Table 6: 5k-path Wilcoxon Test

5.2 Testing for Stage II

Our SDE Eq (4) assumes a bivariate normal distribution generated by dW_t and dZ_t, two Wiener processes underlying IV and IC observables with an instantaneous and constant correlation parameter ρ_w. We now examine the normality of the model derived Brownian increments.

First we present the density function plots with a normal curve overlay, labeled as Normality Test (1) in Fig (6). We observe a very mild case of fat-tail (leptokurtic) in distributions of dW_t and dZ_t.

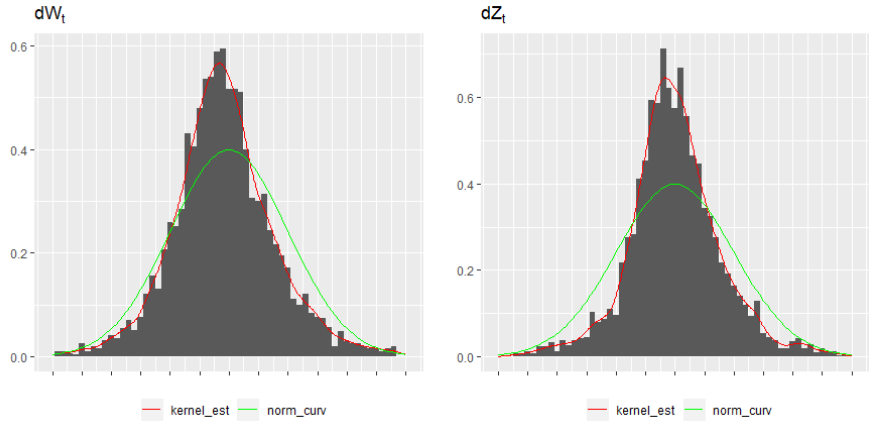

Figure (6): dW_t and dZ_t Normality Tests (1)

Normality Test (2) is consisted of a pair of QQ-plots and ACF autocorrelation graphs. Fig (7) suggest the fact that a wide-ranged linearity and low autocorrelation have been tested in the time series of estimated residual, in support of the Gaussian distribution assumptions for dW_t and dZ_t.

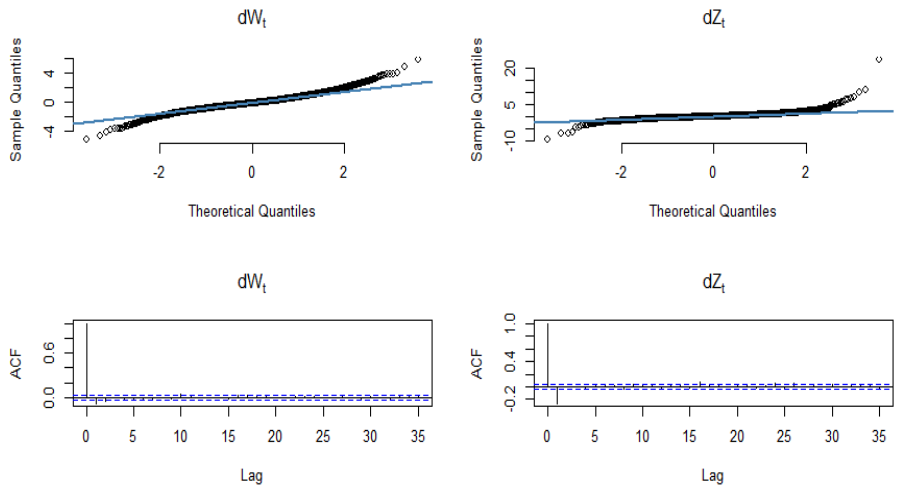

Figure (7): dW_t and dZ_t Normality Tests (2)

With a reasonably high degree of confidence in normality, we conclude that our proposed Stage II calibration method for ρ_w is consistent with empirical evidence.

5.3 Testing the Joint Distribution of IV and IC

Clearly Fig (2a) makes a strong case in support of our USVSC model, as it successfully captures the very key feature of the real word implied volatility-correlation relationship as depicted by Fig (1a).

To statistically measure the fit, we apply Fisher's Z-transformation to test the Pearson correlation difference of two un-paired independent samples: one is the historical realization sample of IV and IC, and the other is estimated from the 5K paths of 2-dimensional simulation of IV and IC.

With a zero correlation difference as the null hypothesis, we obtain a Z-Score of 1.59 reported in Table 7. This test statistics indicates that the Pearson correlation estimation, between simulated IV and IC, is indistinguishable in distribution from that of the empirical observed IV and IC, over the sampled time period, at 95% confidence level.

$$H_0\colon \rho_{(IV,IC)} = \hat{\rho}_{(\widehat{IV},\widehat{IC})}$$

Z	1.5900
2-Tailed Prob	0.1118

Table 7: IV and IC Dependency Test

We, therefore, conclude that the empirical joint distribution of IV and IC is replicated by our proposed USVSC model with sufficient accuracy.

6. Application of the Model – An enhanced Geometric Brownian Motion

With the stochastic IV and IC fully parameterized and tested, we can now re-visit GBM model log-normal specification in Eq (1), the most foundational claim of the asset price returns in the finance literature.

Using GBM as the benchmark, Eq (1) parameters {μ, σ} are first calibrated through MLE. Table 8 gives the estimation results along with the corresponding standard errors.

	coeff	std error
μ	-0.0007	0.0817
σ	0.2897	0.0036

Table 8: Eq (1) GBM Model Calibration

Although the calibrated spot price volatility σ under GBM is robust and statistically significant, the same conclusion may not be drawn with respect to the parameter μ. The large estimation error suggests that the null hypothesis (μ=0) is rather unrejectable with confidence, a subject to which we will return later.

Integrating our stochastic local volatility and correlation model, we proceed to replacing the constant diffusion coefficient σ with our time-varying and stochastic IV denoted by σ_t, as defined in Eq (2). The GBM Eq (1) thereby evolves into Eq (1a) - enhanced-GBM model, allowing the cash spot market infused with additional information sourced from the derivatives market:

$$dS_t/S_t = \mu\, dt + \sigma_t dB'_t \qquad (1a)$$

where dB'_t denotes a new Brownian motion for price returns, distinct from the original dB_t from Eq (1).

To incorporate the proposed USVSC model, we further assume that the risk factors inherent to IV and IC markets are also integral to the dynamics of index trading, therefore can be thought of as priced state variables for asset pricing. This is not unreasonable, as the derivatives IV and IC have become standalone asset classes, albeit with a shorter history and a narrower investor base relative to the underlying cash market. VIX, for example, has evolved from being a latent risk parameter to a set of publically investable trading product group largely helped by the creation of VIX Index and VIX futures commenced in 2004. Not unexpectedly, the stochasticity of IC is argued by Emmerich [20] as a fundamental source of risk, which is furthered by Driessen et al. [18] in a hunt for risk premium in the context of asset pricing. The roles of derivatives markets affecting index price discovering and the broader market have become more evident recently. Details and in-depth discussions on the market structure of VIX fixing, dispersion and worst-of option pricing, can be found in Osterrieder et al. [34], Li [28] and Zetocha [36].

Across three stylized state variables, i.e. the Brownian motion increments dB'_t together with dW_t and dZ_t, a deterministic dependence structure is superimposed. This is manifested by Eq (10) and Eq (11) sequentially, with ρ_B and ρ_Z denoting the instantaneous correlation coefficients between spot-IV and spot-IC, respectively.

Since dW_t and dZ_t are interconnected through ρ_w, as previously established by Eq (4), one can write:

$$dZ_t = \rho_w \, dW_t + \sqrt{1 - \rho_w^2} \, dW'_t \tag{10}$$

with $W_t \perp W'_t$ as usual. Helped with the introduction of a third orthogonal factor $W_t^{"}$, we can now decompose the Weiner process dB'_t in a 3-independent-factor representation:

$$\mathrm{d}B_t' = \rho_B\ \mathrm{dW_t} + \frac{\rho_Z - \rho_w\,\rho_B}{\sqrt{1-\rho_w^2}}\mathrm{d}W_t' + \sqrt{1-\rho_B^2-\frac{(\rho_Z-\rho_w\,\rho_B)^2}{\sqrt{1-\rho_w^2}}}\,\mathrm{d}W_t^{"} \quad (11)$$

So that the recoveries of $\rho_B = \mathrm{E}\,(\mathrm{dB_t^{'}} \times \mathrm{dW_t})\,/\mathrm{dt}$, $\rho_Z = \mathrm{E}\,(\mathrm{dB_t^{'}} \times \mathrm{dZ_t})\,/\mathrm{dt}$ and the identity property of $\mathrm{E}\,(\mathrm{dB_t^{'}} \times \mathrm{dB_t^{'}})\,/\mathrm{dt} = 1$ are satisfied. This particular setup should allow us to exploit the connections between index price dynamics with IV and IC observables[7].

It should be noted that by now $\mathrm{dW_t}$ and $\mathrm{dZ_t}$ have been attained from calibration Stage II. Therefore $\mathrm{d}W_t'$ and $\mathrm{d}W_t'$ are the two added sources of independent Gaussian white noise under the newly enhanced-GBM model Eq (1a).

Our task is therefore reduced to estimating the drift μ and correlation coefficients ρ_B and ρ_Z, and testing if the enhanced-GBM Eq (1a) is valid given our model setting. We proceed as follows.

Let $x_t = \ln(S_t)$ to simplify the notation for asset price returns, after applying Ito's lemma, Eq (1a) is expanded to a 3-factor model Eq (1b), admitting the information transformation from IV and IC markets rather explicitly:

$$d\mathrm{x_t} = \left(\mu - \frac{1}{2}\sigma_t^2\right)\mathrm{dt} + \sigma_t\left(\rho_B\ \mathrm{dW_t} + \frac{\rho_Z - \rho_w\,\rho_B}{\sqrt{1-\rho_w^2}}\mathrm{d}W_t' + \sqrt{1-\rho_B^2-\frac{(\rho_Z-\rho_w\,\rho_B)^2}{\sqrt{1-\rho_w^2}}}\,\mathrm{d}W_t^{"}\right) \quad (1b)$$

Taking the expectations on both sides, aided by the assumed Gaussianity of $\{\mathrm{d}W_t, \mathrm{d}W_t', dW_t^{"}\} \sim \mathrm{N}(0,\mathrm{dt})$, we arrive at the drift rate estimator

$$\hat{\mu} = \mathrm{E}[\frac{dx_t}{dt} + \frac{1}{2}\sigma_t^2] \quad (12)$$

[7] By this design, the risk transmission from IV into spot market is channeled through correlated Brownian motions, as the stochastic σ_t in Eq (1a) is set to historical observations directly. For additional insights of CKLS, readers are referred to Chan et al. [13] and Hu et al. [25].

Where all RHS variables are known, we obtain a calibration result and a statistical inference test in Table 9. At 95% confidence level, the null is once again unrejectable - same conclusion under the original GBM model. We thereby argue that the constant drift assumption under GBM (1) or (1a) is unsupported by the sampled historical data. That is, the linear drift term under GBM is not robust and likely misspecified, irrespective of the diffusion term being constant or locally stochastic.

$H_0: \mu = 0$	
μ	0.10803
T	1.35320
p-value	0.17610

Table 9: GBM (1a) Calibration and Inference Test of Drift μ

It is clear now that the calibration of ρ_B and ρ_z is equivalent to locating the maximization of the log-likelihood (LL) function of a standard normal density over the full historical data sample:

$$\frac{dW_t'}{\sqrt{dt}} = \frac{\sqrt{dt}\,\sigma_t\,(\rho_z - \rho_B\rho_w)}{(dx_t + \frac{1}{2}\sigma_t^2 dt - \mu dt)\sqrt{1-\rho_w^2}} \quad \sim N(0,1) \tag{13}$$

Fig (8) pictorializes the calibration approach. The optimal solution is simply the coordinates of ρ_B and ρ_z, on a squared region of [-1, +1], at which the inverse of the Log-Likelihood (LL) function reaches a global minimum.

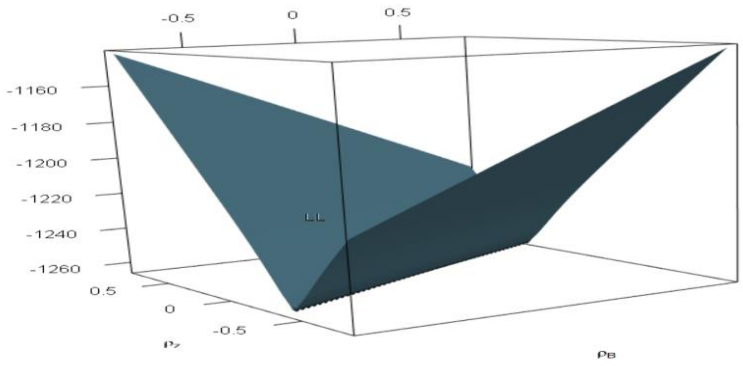

Figure (8): MLE Solving ρ_B and ρ_z

An implementation for a non-linear optimization algorithm yields a solution pair of $\widehat{\rho_B}$ and $\widehat{\rho_z}$, displayed in a matrix form in Table 10 together with the estimated $\widehat{\rho_w}$ for completeness:

$$\begin{bmatrix} 1 & & \\ \widehat{\rho_w} & 1 & \\ \widehat{\rho_B} & \widehat{\rho_Z} & 1 \end{bmatrix} = \begin{bmatrix} 1 & & \\ +0.5056435 & 1 & \\ -0.5852176 & -0.2959115 & 1 \end{bmatrix}$$

Table 10: Correlation Matrix

The estimated negative correlation $\widehat{\rho_B}$, between spot and IV, corroborates the leverage effect puzzle termed by Ait-Sahalia et al. [4], and converges with the results by Zetocha [36]. This is also a widely known phenomenon by retail investors, as described in CBOE [12].

The negative correlation $\widehat{\rho_z}$, between spot and IC, comes as no big surprises as stock prices tend to correlate more as the market is down than the reverse, consistent with a unique and well-known IC market feature - *correlation skew* by Reghai [35], Zetocha [36] and Delanoe [17]. In the academic literature, however, the interactivities of spot-IC have not been extensively studied relative to spot-IV.

Several normality tests undertaken for $\frac{dB_t}{\sqrt{dt}}$ estimated under GBM (1), as well as $\frac{dB_t'}{\sqrt{dt}}$ under GBM (1a): Table 11 gives the numerical improvements in Jargue Bera statistics; Fig (9) charts the normalized density plots benchmarked against the standard normal; Fig (10) supplements QQ-plots. The substantial gains in performance, of our joint stochastic Implied Volatility and Implied Correlation model over the original GBM model, are demonstratively significant.

$$H_0: \quad \left\{\frac{dB_t}{\sqrt{dt}}, \frac{dB_t'}{\sqrt{dt}}\right\} \sim N(0,1)$$

	GBM (1)	GBM (1a)
Jarque Bera	15596	41.013

Table 11: GBM Normality Test

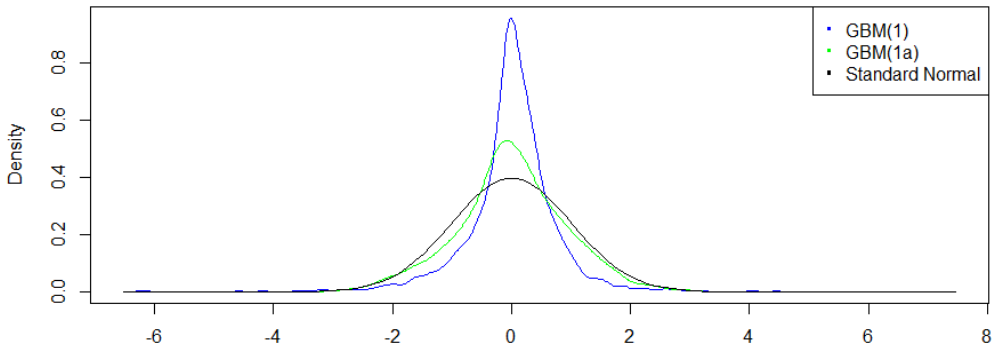

Figure (9): Density Distribution Comparison

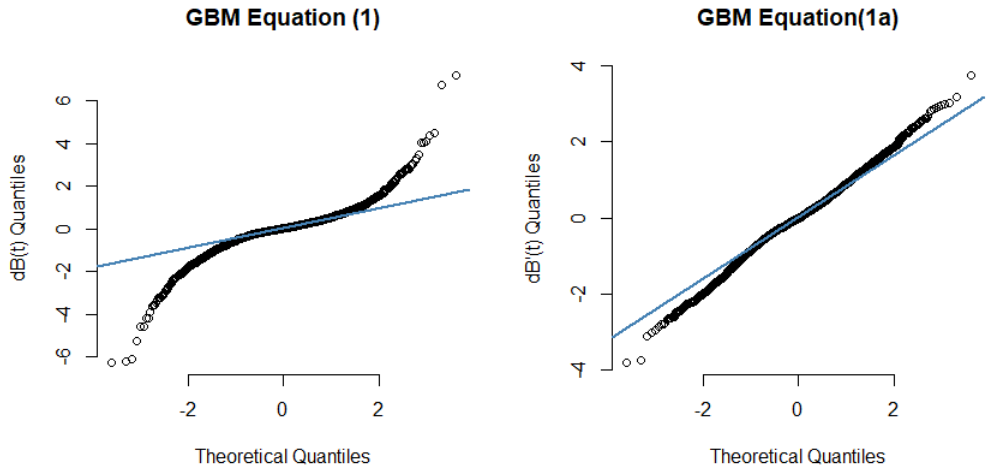

Figure (10): QQ-plot Comparison

7. Concluding Summary

The dynamics of asset prices is typically modeled by stochastic processes, however their correlations are exogenously modeled and ad hoc assigned to the price process. This is mathematically and conceptually unsatisfying.

We propose a simple and unified framework to model local stochastic volatility and local stochastic correlation, similar to the approach by Heston [23]. Powered by

coupled CIRCEV and Jacobi processes, our structural USVSC model is parsimonious and capable of re-producing the non-trivial volatility and correlation skews observed in the real world. The calibration scheme developed is intuitive and tractable, with results proven significant. The goodness of fit is backed by robust inference results after undertaking multiple stringent statistical tests in both *marginal* and *joint* distributions of the implied volatility and implied correlation.

We show our well-calibrated model performs demonstrably better over the classical GBM approach, thus a suitable and practical challenger for asset pricing, especially under current market structure. We highlight and quantify a number of unique properties of Implied Correlation: it strongly co-moves with Implied Volatility, but counters to the direction of price shocks, as does the Implied Volatility, albeit the connection to spot is markedly weaker in comparison. In addition to `Delta' and `Vega' risk terms, we prove that the dynamics of Implied Correlation exhibit a greater irreducibility relative to Implied Volatility, hence a unique source of randomness in the financial system.

Future research of our USVSC model may entail analyzing the sensitivity and stability to historical data sampling periods, and testing its capabilities in fitting the volatility smiles, term structure and correlation skews, for the purpose of pricing basket options and risk management. Additionally, new trading strategies may be developed if the equity option-implied correlation skews have awareness of the CDO tranche - implied correlation skews, across firm capital structure and asset classes. Lastly, placing the implied correlation and joint dynamics of volatility-correlation in a wider context of risk premium study should add useful insights in the field of financial economics.

References

1. Ahdida, A., Alfonsi A.: A mean-reverting SDE on correlation matrices. Stochastic Processes ad their Applications 123, 1472-1520 (2013)

2. Ait-Sahalia, Y.: Maximum Likelihood Estimation of Discretely Sampled Diffusions: a Closed - Form Approximation Approach. Econometrica, 70 (1), 223-262 (2002)

3. Ait-Sahalia, Y., Kimmel, R.: Maximum Likelihood Estimation of Stochastic Volatility Models. Journal of Financial Economics, 83 (2), 413-452 (2007)

4. Ait-Sahalia, Y., Fan, J., Li, Y.: The Leverage Effect Puzzle: Disentangling Sources of Bias at High Frequency. Journal of Financial Economics, 109 (1), 224-249 (2013)

5. Bergomi, L.: Smile Dynamics II, Risk, October (2005)

6. Brigo, C., Pallacinini, A.: Counterparty Risk and CCDSs under Correlation. Risk, 21, 84-88 (2008)

7. Bu, R., Cheng, J., Hadri, K.: Specification Analysis in Regime-switching Continuous-time Diffusion Models for Market Volatility. Studies in Nonlinear Dynamics & Econometrics, 21 (1), 65-80 (2017)

8. Buraschi, A., Porchia, P., Trojani, F.: Correlation Risk and Optimal Portfolio Choice. Journal of Finance, 65, 392-420 (2010)

9. Burtschell, X., Gregory, J., Laurent, J-P.: Beyond the Gaussian Copula: Stochastic and Local Correlation. Journal of Credit Risk, 3(1), 31-62 (2007)

10. CBOE White Paper: CBOE Volatility Index (2019)

11. CBOE: CBOE S&P 500 Implied Correlation Index (2009)

12. CBOE: The Relationship of the SPX and the VIX® Index (2012)

13. Chan, K., Karolyi, A., Longstaff, F., Sanders, A.: An Empirical Comparison of Alternative Models of the Short-term Interest Rate. Journal of Finance, 47 (3), 1209-1227 (1992)

14. Cont, R., Fonseca, J.: Dynamics of Implied Volatility Surfaces. Quantitative Finance, 2, 45-60 (2002)

15. Cont, R., Kokholm, T.: A Consistent Pricing Model for Index Options and Volatility Derivatives. Mathematical Finance, 23 (2), 248-274 (2013)

16. Cox, C., Ross, S.: The Valuation of Option for Alternative Stochastic Processes. Journal of Financial Economics, 3(1-2), 145-166 (1976)

17. Delanoe, P.: Local Correlation with Local Vol and Stochastic Vol. SSRN:2454668 (2014)

18. Driessen, J., Maenhout, P., Vilkov, G.: Option-Implied Correlations and the Price of Correlation Risk. Advanced Risk & Portfolio Management Paper, SSRN:2166829 (2005)

19. Düllmann, K., Kull, J., Kunisch, M.: Estimating Asset Correlations from Stock Prices or Default Rates - Which Method is Superior? Deutsche Bundesbank Working Paper (2008)

20. Emmerich, C.: Modeling Correlation as a Stochastic Process. Bergische Universitaet Wuppertal Working paper (2006)

21. Fonseca, J., Graselli, M., Ielpo, F.: Estimating the Wishart Affine Stochastic Correlation Model Using the Empirical Characteristic Function. SSRN:1054721 (2008)

22. Hagan, P. S., Kumar, D., Lesniewski, A., Woodward, D.: Managing Smile Risk. Wilmott, 1, 84-108 (2002)

23. Heston, S.: A Closed-Form Solution for Options with Stochastic Volatility with Applications to Bond and Currency Options. The Review of Financial Studies, 6, 327-343 (1993)

24. Hollstein, F., Prokopszuk,M., Wese Simen, C.:The Term Stuture of Systematic and Idiosyncratic Risk, Hannover Economic Papers (HEP), No. 618 (2017)

25. Hu, Y., Lan, G., Zhang, C.: The Explicit Solution and Precise Distribution of CKLS Model under Girsanov Transform. arXiv:1410.2364 (2014)

26. Hull, J., Predescu, M., White, A.: The Valuation of Correlation-Dependent Credit Derivatives using a Structural Model. Journal of Credit Risk. 6 (3), 99–132 (2005)

27. Langnau, A.: Introduction into Local Correlation Modelling, Allianz SE and LMU Munch working paper. arXiv:0909.3441 (2009)

28. Li, A.: Improvements to the CBOE VIX Calculation Formula. SSRN:2991829 (2017)

29. Ma, J.: Pricing Foreign Equity Options with Stochastic Correlation and Stochastic Volatility. Annals of Economics and Finance, 10-2, 303–327 (2009a)

30. Ma, J.: A Stochastic Correlation Model with Mean Reversion for Pricing Multi-Asset Options. Asia-Pacific Financial Markets, 16 (2), 97-109 (2009b)

31. Madan, D., Carr, P., Chang, E.: The Variance Gamma Process and Option Pricing. Review of Finance, 2(1), 79-105 (1998)

32. Meissner, G., “Correlation Risk Modeling and Management”, RISKbooks (2019)

33. Merton, R.C.: Option pricing when the Underlying Stock Returns are Discontinuous. Journal of Financial Economics, 3, 125-144 (1976)

34. Osterrieder, J., Roschli, K., Vetter, L.: The VIX Volatility Index - A Very Thorough Look at It. SSRN:3311727 (2019)

35. Reghai, A.: Breaking Correlation Breaks. Risk, October 90-95 (2010)

36. Zetocha, V.: Skewing Up Correlation: Understanding Correlation Skew in Equity Derivatives. SSRN:2441724 (2014)

37. Zhou, C.: An Analysis of Default Correlations and Multiple Defaults. The Review of Financial Studies, 14, 555-576 (2001)